JTTEE5 16:404–413
DOI: 10.1007/s11666-007-9046-3
1059-9630/$19.00 © ASM International

Peer Reviewed

MoB/CoCr Cermet Coatings by HVOF Spraying against Erosion by Molten Al-Zn Alloy

Hiroaki Mizuno and Junya Kitamura

(Submitted September 27, 2006; in revised form January 11, 2007)

MoB/CoCr, a novel cermet material for thermal spraying, with high durability in molten alloys has been developed to utilize for aluminum die-casting parts, and for hot continuous dipping rolls in Zn and Al-Zn plating lines. The durability of the MoB/CoCr coatings prepared by high velocity oxy-fuel (HVOF) spraying has been investigated using a molten-metal immersion tester. The tests revealed that the MoB/CoCr coating has much higher durability without dissolution in the molten Al-45wt.%Zn alloy. Little change of crystal structure, mainly composed of double borides of CoMoB and $CoMo_2B_2$, is observed after the immersion test, suggesting that the double borides have much higher durability. Using undercoat is effective to reduce the influence of large difference in thermal expansion between the MoB/CoCr topcoat and substrate of stainless steel of AISI 316L, widely used for the hot continuous dipping rolls. Optimized thickness combinations of topcoat and undercoat are necessary to obtain intrinsic performance of low reactive MoB/CoCr against the molten Al-45wt.%Zn alloy.

Keywords cermet coatings, coefficient of thermal expansion, erosion and abrasion resistance, high temperature erosion, novel material, thermal shock

1. Introduction

Thermal spray coatings offer some customized surface properties, such as resistance to corrosive atmosphere, abrasion, erosion, high temperature, and high heat flux. Recently, these properties of the spray coatings have been greatly progressed by development of novel spray equipments, such as high-power plasma spraying and high velocity oxygen-fuel (HVOF) spraying (Ref 1, 2), as well as by development of feedstock (Ref 1) including customization for the equipments. Thus, the applications of spray coatings can be expanded by the development. Durable spray coatings in molten metals are one of the possible applications, for example (Ref 3). Improvement of hot continuous dipping parts, such as sink rolls and stabilizing rolls, with higher erosion resistance against molten zinc (Zn) and aluminum-zinc (Al-Zn) alloys is one of the key issues in steel manufacturing process (Ref 4). It is considered that rolls coated by Co-based self-fluxing alloy has insufficient durability in spite of relatively longer life compared to the common roll made from stainless cast steel (Ref 5, 6).

Some groups have reported that WC/Co coatings prepared by the HVOF spraying show higher durability than the Co-based alloy coating in molten pure Zn (Ref 5) and Al-Zn (low Al content) alloys (Ref 6). Inclusion of double carbides of η-phase (Co_3W_3C and Co_6W_6C) in the WC/Co coating is found to be effective to improve the durability, where η-phase reduces free metal Co with high reactivity (Ref 5-8). However, surface modifications without adhesion of the molten alloy and dissolution by the alloy are still required by the steel manufacturers to increase the operating time retaining the product quality. In addition, the effect of the η-phase coating is only limited for the molten alloys at relatively lower temperature of less than 750 K. Since Al-rich Al-Zn alloy plating lines, Al-45wt.%Zn for example, are generally operated at higher temperature of more than 900 K, the condition becomes serious and it is difficult to apply the spray coatings onto hot continuous dipping parts, in general. No development of the coating material suitable for such a serious condition is reported, as far as we know.

Recently, a novel thermal spray material of MoB/CoCr with higher durability against molten Al and Al-Zn alloys has been developed by Fujimi Incorporated (Japan) to utilize for die casting parts and for hot continuous dipping parts (Ref 9-11). The durability of the MoB/CoCr coatings prepared by the HVOF spraying has been investigated using a laboratory-scaled molten-metal immersion tester. The basic immersion test has revealed that the MoB/CoCr coating has much higher durability in the molten Al and Al-Zn alloys than conventional spray coatings. Further, no damage or dissolution are observed in the MoB/CoCr coating after long-term immersion test of molten Al-45wt.%Zn alloy, where both the conventional cermet and ceramic coatings are damaged due to dissolution and crack generation, respectively. However, influence of the coating structure, which may affect the lifetime of the

Hiroaki Mizuno and **Junya Kitamura,** Thermal Spray Materials Department, Fujimi Incorporated, Kakamigahara, Gifu Pref., 509-0103, Japan. Contact e-mail: mizunoha@fujimiinc.co.jp.

dipping rolls drastically, is still unclear. Especially, no examination has been conducted using stainless steel of AISI 316L as substrate, whose material is mainly used as a sink roll and stabilizing rolls in actual Al-rich Al-Zn plating lines.

In this article, potential of MoB/CoCr coatings for Al-45wt.%Zn plating line has been investigated through laboratory-scaled molten-metal immersion tests. Also, coating structures, in terms of base substrate, its coefficient of thermal expansion (CTE) and thickness of undercoat and topcoat, have been studied to avoid crack generation in the coating and peel off of the coating, whose damages can drastically reduce the lifetime of the coated parts, in spite of high durability (low reactivity) of MoB/CoCr against the molten Al-Zn alloy.

2. Experimental

2.1 Structural, Chemical, and Mechanical Analysis of the Powders and the Spray Coatings

Micro-structural analysis was conducted using a scanning electron microscopy (SEM: SEMEDX III, Hitachi-High Technologies Corp., Japan) and an optical microscopy. Porosities of the spray coatings were estimated by an imaging analysis using the optical microscope. Energy dispersive x-ray (EDX: EX-250SE, HORIBA Ltd., Japan) analysis was used for chemical analysis. Crystal structures of the powders and the coatings were identified from x-ray diffraction analysis (XRD: RINT-2000, RIGAKU Corp., Japan). Hardness of the coatings was measured using micro Vickers hardness tester (HMV-1, SHIMADZU Corp., Japan), whose indenting load was 1.96 N and loading time was 10 s. Volume wear ratio of the coatings was investigated using Suga abrasion tester (NUS-ISO-3, Suga test instruments Co., Ltd., Japan), whose load was 30.9 N and counter material was abrasive paper of SiC F180, where volume loss of carbon steel (JIS SS400) was used as a reference.

2.2 Preparation of MoB/CoCr Powder

Commercially available fine powders of molybdenum boride, chromium boride, and cobalt-based alloy (Co-30 wt.% Cr-4 wt.% W-1.2 wt.% C) as raw materials were mixed and milled in solvent by ball milling. The milled powder was agglomerated using spray drier. The agglomerated powders were sintered at more than 1273 K in inert gas to form double borides of Co-Mo-B by a chemical reaction of metal borides and cobalt-based alloy. After sintering process, particle size distribution of the MoB/CoCr was optimized for HVOF spraying through classification process. The particle size distribution and typical atomic contents are shown in Table 1. Figure 1 shows an x-ray diffraction (XRD) pattern for the MoB/CoCr powder after sintering process. The MoB/CoCr powder is mainly composed of double borides of both $CoMo_2B_2$ and CoMoB. An SEM image and element mappings by the EDX analysis of the MoB/CoCr powders are shown in Fig. 2.

Table 1 Characteristics of MoB/CoCr powder

Powder manufacturing method	Agglomerated and sintered				
Particle size	−45 + 15 μm				
Chemical composition, wt.%	Mo	Co	Cr	B	W
	Bal.	22.5	19.1	8.5	1.6

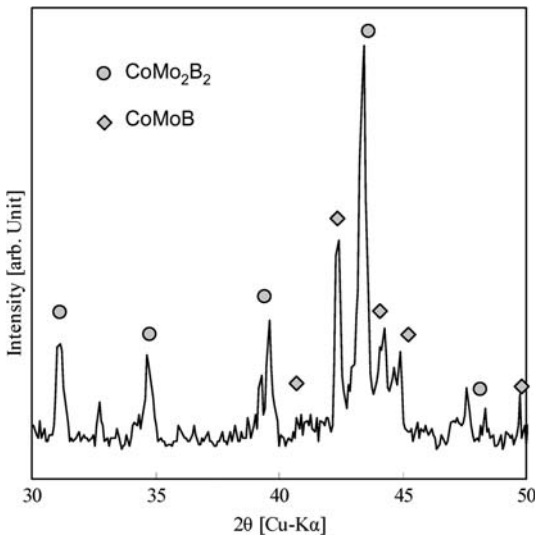

Fig. 1 An x-ray diffraction pattern for the MoB/CoCr powder

2.3 Measurement of Coefficient of Thermal Expansion (CTE)

Coefficient of thermal expansion (CTE) of the spray coatings and substrate materials was measured by thermomechanical analyzer (Thermo Plus TMA-8310, RIGAKU Corp., Japan). The spray coatings were prepared onto steel plate (JIS SS400, $50\times70\times2^t$ mm), where thickness of the coating was set to about 500 μm. The specimens were also used for the XRD analysis. As for thermodilatometry, the coatings were separated from the substrate using a micro-cutting machine. The separated coatings were cut about the size of $5\times20\times0.5^t$ mm and the CTE was measured in-plane direction. The heating and cooling rate was 5 K/min in argon gas and heating-cooling cycle was repeated three times from 323 to 1273 K. The CTE of each specimen was estimated from the second heating cycle data. In this article, temperature range of the CTE was set to 373-923 K.

2.4 Preparation of Thermal Spray Coatings for Molten Al-45wt.%Zn Alloy Immersion Test

Table 2 summarizes the specimens for the molten Al-45wt.%Zn alloy immersion test, where the measured CTE of the spray coatings (topcoat and undercoat) and substrates are described. Conventional ceramics of white alumina (PS-A, product name: SURPREX AW50) and yttria stabilized zirconia (PS-Z, prototype name: DTS-Z10-45/10) as well as a conventional cermet of WC/12 wt.% Co (HV-W1, product name: SURPREX WC12J)

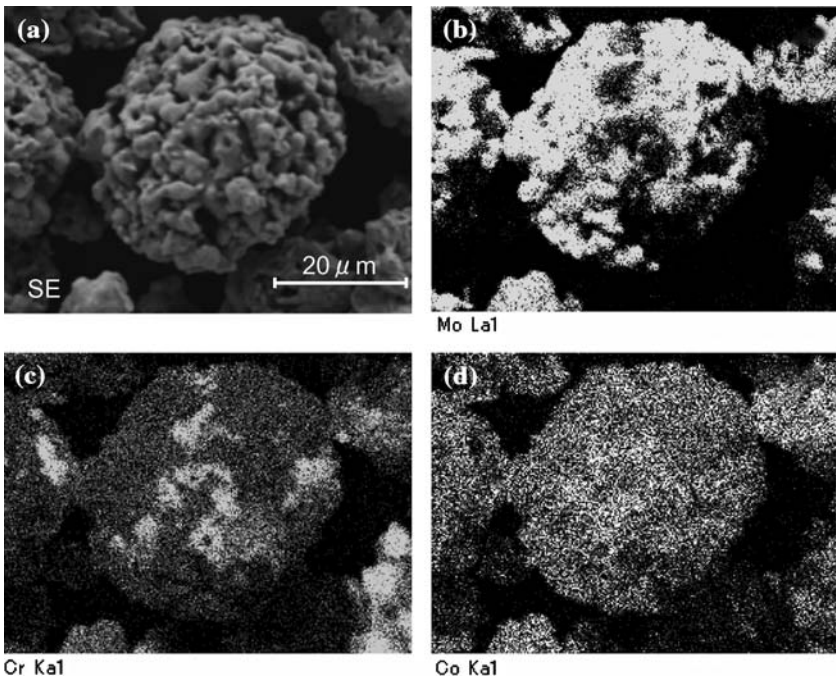

Fig. 2 (a) An SEM image and element mappings of (b) Mo, (c) Cr, and (d) Co of the MoB/CoCr powder

Table 2 Specimens for the molten Al-45wt.%Zn immersion test

		Topcoat		Undercoat	
No.	**Substrate**	**Materials/CTE**	**Thickness**	**Materials/CTE**	**Thickness**
PS-A	AISI H13/12.7×10^{-6}	Al_2O_3/7.8×10^{-6}	150 μm	Without	...
PS-Z		ZrO_2-8wt.%Y_2O_3/10.4×10^{-6}			
HV-W1		WC/12 wt.% Co/7.2×10^{-6}			
HV-W2		WC/12 wt.% Co(low carbon)/6.8×10^{-6}			
HV-B1		MoB/CoCr/9.2×10^{-6}			
HV-B2	AISI 316L/19.3×10^{-6}				
HV-B3				AISI 440C/12.4×10^{-6}	50 μm
HV-B4				Co-30wt.% Cr-4wt.%	
HV-B5				W-1.2wt.%C/15.0×10^{-6}	100 μm
HV-B6			100 μm		50 μm
HV-B7					500 μm

powders are manufactured by Fujimi Incorporated, Japan. The MoB/CoCr powder (from HV-B1 to B7, prototype name: DTS-B49-45/15) also has been developed by Fujimi Incorporated.

Two steels were used as substrates, whose size was φ19 mm×200 mm with a round-shaped nose, as shown in Fig. 3(a). Lower CTE one is AISI H13 (Fe-0.37C-5.0Cr-1.3Mo-1.0Si-1.0V, 12.7×10^{-6}/K), which is a typical material of the mold for aluminum die-casting. The specimens from PS-A to HV-B1 were sprayed onto the AISI H13 to evaluate mainly the dissolubility of these coatings in the molten Al-45wt.%Zn alloy because the CTE difference between the coatings and the substrate was relatively smaller that should reduce the damage by thermal shock, such as crack generation and peel off.

PS-A (alumina, Al_2O_3) and PS-Z (yttria stabilized zirconia, ZrO_2-8wt.%Y_2O_3) have been prepared by plasma spraying whose conditions are summarized in Table 3. The CTE of each coating was 7.8×10^{-6}/K and 10.4×10^{-6}/K, respectively. The other specimens are HVOF sprayed coatings whose spray conditions are also summarized in Table 3. All substrates were sand-blasted using alumina grit of F40 before spraying. HV-W2 (6.8×10^{-6}/K), prepared on trial, was basically same as HV-W1 (7.2×10^{-6}/K) of conventional WC cermet, except for using WC with lower carbon content. When low carbon WC is sintered with Co, double carbides, such as η-phase (Co_3W_3C and Co_6W_6C), are generally formed. Carbon contents in the HV-W1 and HV-W2 powders were 5.5 and 4.2 wt.%, respectively. HV-B1 was the MoB/CoCr coating (9.2×10^{-6}/K) onto the AISI H13 substrate.

Stainless steel of AISI 316L with higher CTE of 19.3×10^{-6} /K compared to AISI H13 was used as substrates for the MoB/CoCr specimens from HV-B2 to

HV-B7. This stainless steel is currently used for conventional continuous dipping rolls due to its relatively high durability against molten Al-45wt.%Zn alloy. As for HV-B2, MoB/CoCr was directly sprayed onto the AISI 316L without undercoat. Undercoat was prepared for the specimens from HV-B3 to HV-B7. AISI 440C coating with the CTE of 12.4×10^{-6}/K was formed as undercoat for the HV-B3. From HV-B4 to HV-B7, Cobalt-based alloy coating with the CTE of 15.0×10^{-6}/K was also prepared as undercoat, where thickness of both the undercoat and the MoB/CoCr topcoat was changed to find the optimal thickness to reduce the negative influence of the considerably large CTE difference between the MoB/CoCr coating and the AISI 316L substrate.

2.5 Immersion Test in the Molten Al-45wt.%Zn Alloy

A schematic of the molten-metal immersion tester designed by Fujimi Incorporated is illustrated in Fig. 4. Specimens were repeatedly immersed in a molten alloy at the constant temperature of 923 K. The specimens were rotating and orbiting in the molten metal to come into contact with a fresh molten metal as well as to preserve liquid uniformity during the test. The dissolubility of specimens against the molten metal and thermal shock resistance were evaluated by using this tester through the repetition of immersing and air cooling. The specimens were automatically photographed by a high-speed camera at the time of cooling operation, and the photograph data was stored into a personal computer. Dissolution or mechanical damage of the specimens was checked by visual observation or stored data, and then the lifetime was estimated.

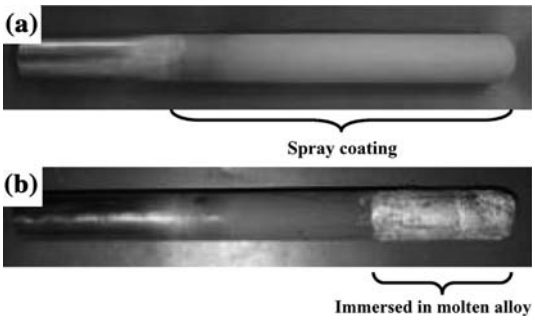

Fig. 3 Photographs of typical specimens of (a) as-sprayed and (b) after immersion test

The experimental conditions of the immersion test in the molten Al-45wt.%Zn are summarized in Table 4. These conditions (alloy composition and its temperature) have been set by assuming that the coatings are applied to the hot continuous dipping rolls, such as sink rolls and stabilizing rolls. Thus, the specimens were repeatedly pulled out from the molten Al-45wt.%Zn for only 1 min to take a photograph by the high-speed camera or to check the specimens visually after long-term immersion of 60 min. Spray coated area was about 120 mm in length from the nose, as shown in Fig. 3(a). Figure 3(b) shows a typical specimen after the immersion test of molten Al-45wt.%Zn alloy, whose immersed length is about 50 mm. Dissolution of the substrate is clearly seen near the round-shaped nose.

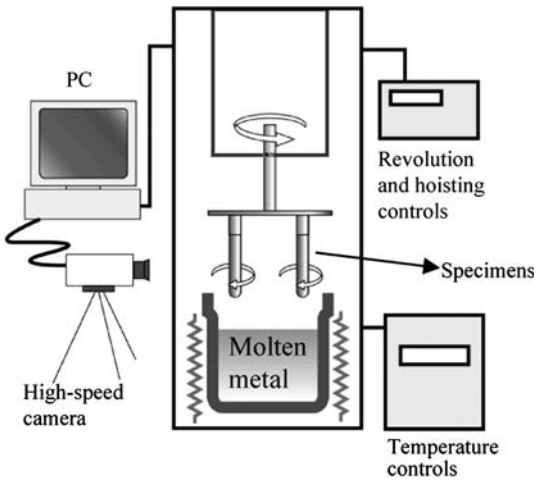

Fig. 4 Schematic of the molten-metal immersion tester

Table 4 Conditions of the molten Al-45wt.%Zn immersion test

Rotation speed	120 rpm
Orbital speed	30 rpm
Immersion time	60 min
Cooling time	1 min
Alloy composition	Al-45wt.%Zn
Temperature	923 K

Table 3 Conditions of HVOF and plasma spraying

	HVOF		Plasma
Gun	JP-5000(PRAXAIR/TAFA)		SG-100(PRAXAIR)
Coating	Topcoat	Undercoat	Topcoat
Spray	Oxygen flow rate: 893 L/min	Oxygen flow rate: 893 L/min	Ar/He flow rate: 39/7.9 L/min
Conditions	Kerosene flow rate: 0.32 L/min	Kerosene flow rate: 0.32 L/min	Ar/He pressure: 0.34/0.34 MPa
	Barrel length: 203.0 mm	Barrel length: 101.5 mm	Arc current/voltage: 900 A/36 V
	Spray distance: 380 mm	Spray distance: 380 mm	Spray distance: 120 mm

3. Results

3.1 Structural and Mechanical Properties of the Spray Coatings

Figure 5 shows cross-sectional optical micrographs of as-sprayed coatings of alumina (PS-A), WC/12 wt.% Co (HV-W1) and MoB/CoCr (HV-B1). It is clear that the cermet coatings by the HVOF spraying have higher density (lower porosity) than the plasma sprayed alumina coating. Porosities by imaging analysis, hardness and volume wear ratio by Suga abrasion test of the coatings in Fig. 5 are summarized in Table 5. In spite of lower hardness, wear resistance of the MoB/CoCr coating is much better than that of the alumina coating, and is almost comparable to Cr_3C_2/25 wt.% NiCr coating by the HVOF spraying. Lower porosity (1.6%) of the MoB/CoCr coating should be better to avoid penetration of the molten alloy.

3.2 Immersion Test in the Molten Al-45wt.%Zn Alloy

The lifetime of the substrates and spray coatings (from PS-A to HV-B1) in the molten Al-45wt.%Zn alloy is shown in Fig. 6, where the substrate was AISI H13 to investigate mainly the reactivity of the coating materials. Spray coated specimens have much longer lifetime of more than 100 h compared to the substrates: 1 h for AISI H13 and 3 h for AISI 316L. The molten Al-45wt.%Zn alloy was quickly dropped off from the surface of the ceramic coatings (PS-A and PS-Z) at cooling cycle during the test that shows their high inertness. However, mechanical damages generated by heat shock, such as cracks, defluxion of fragment and peel off, were clearly observed visually at about 5 h prior to the dissolution of the base substrates (lifetime). Thus, in spite of their inertness, the lifetime of the ceramic coatings becomes short due to their brittleness and it is clear that the ceramic coatings are difficult to apply to the actual application. As the ZrO_2-8 wt.% Y_2O_3 coating (PS-Z) has the comparatively higher CTE as well as higher toughness than the Al_2O_3 coating (PS-A), it may result in longer lifetime.

The molten alloy was also dropped from the surface up to 100 h for the WC/12 wt.% Co coating (HV-W1). And then, adhesion increased gradually after 100-h immersion and the dissolution of the substrate was observed at 209 h. The HV-W2 (WC/12 wt.% Co with lower carbon content) coating showed higher durability. In spite of adhesion of the alloy onto these cermet coatings suggesting higher reactivity than ceramics, the lifetime is almost comparable to that of the ceramic coatings showing higher heat-shock resistance. The MoB/CoCr coating (HV-B1) has shown excellent durability in the Al-45wt.%Zn alloy without dissolution and mechanical damage even after 623-h immersion.

3.3 Micro-structural Analysis of the Coatings after the Immersion Test

Figure 7 shows cross-sectional SEM images at immersed region after the test. As for damaged specimens

Table 5 Structural and mechanical properties of the thermal spray coatings

	PS-A Al_2O_3	HV-W1 WC/12 wt.% Co	HV-B1 MoB/CoCr
Porosity, %	10.4	2.5	1.6
Vickers Hardness	928	1281	845
Volume wear ratio	1.30	0.03	0.25

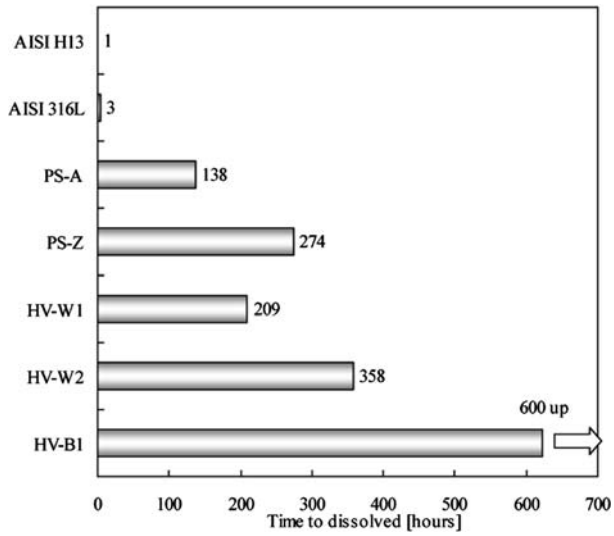

Fig. 6 Lifetime of the specimens coated onto AISI H13 in the molten Al-45wt.%Zn. The MoB/CoCr coating (HV-B1) shows no damage after the 623-h immersion test

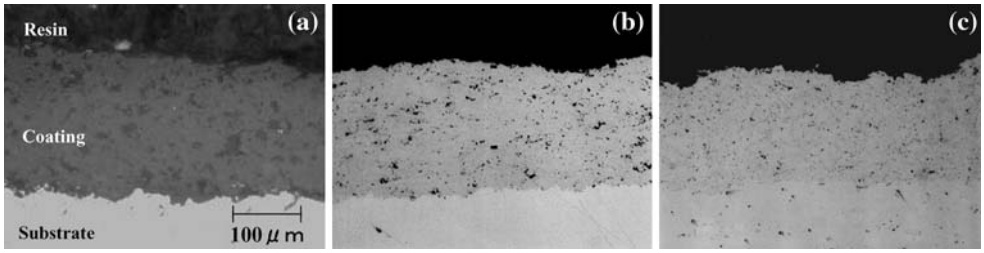

Fig. 5 Cross-sectional optical micrographs of the coatings of (a) alumina (PS-A), (b) WC/12 wt.% Co (HV-W1), and (c) MoB/CoCr (HV-B1) before the immersion test

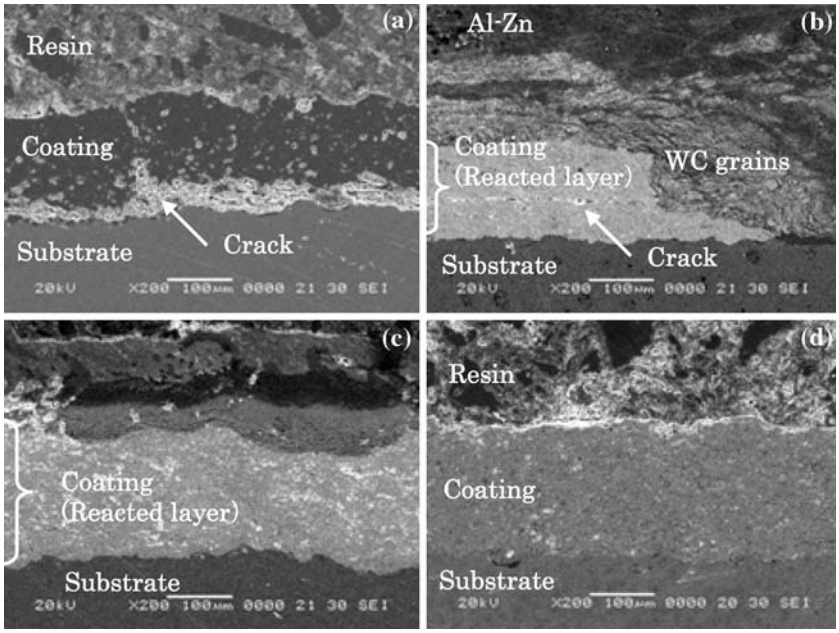

Fig. 7 Cross-sectional SEM images of the coatings after the immersion test in the molten Al-45wt.%Zn alloy. (a) Al_2O_3 (PS-A, 138 h), (b) WC/12 wt.% Co (HV-W1, 209 h), (c) WC/12 wt.% Co with low carbon (HV-W2, 358 h), (d) MoB/CoCr (HV-B1, 623 h)

shown in Fig. 7(a-c), adjacent region of the dissolved region was observed to investigate behavior of damage, such as dissolution, reaction, and mechanical damage. In Fig. 7(a), the Al_2O_3 coating is peeled from the substrate with vertical crack in the coating. No adhesion of the alloy and no reaction layer between Al_2O_3 and Al-Zn alloy are observed, which is identified from the EDX analysis. Considering that the observation of peeling, visible cracks and defluxion of the fragment, mechanical damage is dominant in the ceramic coatings, not dissolution. Therefore, it is considered that the specimen is finally dissolved by contact with the highly reactive steel substrate and the molten Al-Zn alloy, which passes through the vertical cracks in the Al_2O_3 coating.

As for the WC/12 wt.% Co coating (HV-W1) in Fig. 7(b), both Al-Zn alloy layer adhered onto the coating surface and the reaction layer containing Al, Zn, W, and Co are observed. This shows diffusion of Al and Zn into the coating. Also, solid solution and/or intermetallic compound composed of Al, Zn, and the metal binder of Co might be generated. A crack is seen in the reaction layer implying the layer is brittle. Further, diffused WC grains from the coating are seen in the Al-Zn adhesion layer. Dissolution behavior of the WC/12 wt.% Co with low carbon coating (HV-W2) in Fig. 7(c) is almost similar to that of the conventional WC/12 wt.% Co coating (HV-W1) except for higher durability, where adhesion of the Al-Zn alloy and mixed layer of Al, Zn, W, and Co are also observed. In the MoB/CoCr coating (HV-B1) in Fig. 7(d), no decrease in the coating thickness and adhesion of the Al-Zn alloy have been found even after the long-term immersion of 623 h.

In order to investigate the dissolution behavior by Al-Zn alloy in detail, line analysis by EDX is conducted as shown in Fig. 8. Adhesion of the Al-Zn alloy, reaction layer composed of Al, Zn and WC are observed on the WC/12 wt.% Co coating, whose thickness are apparently decreased, as shown in Fig. 8(a). It is found that diffusion behavior between Al and Zn is different identified from the line profiles. Al intensity is higher in the Al-Zn adhesion and decreases sharply at the interface between the adhesion and the reaction layer. Further, it is almost comparable to background intensity in the WC/12 wt.% Co coating showing that Al is included in the adhesion and the reaction layer. On the other hand, in addition to the adhesion and the reaction layer, Zn is also detected in the WC/12 wt.% Co coating showing that diffusion of Zn is faster than that of Al. Gradual diffusion of Zn is also different from the stepped diffusion of Al. Al and Zn intensities are almost comparable to background intensities that shows no or little diffusion of both Al and Zn into the MoB/CoCr coating as shown in Fig. 8(b).

3.4 Crystal Structural Analysis of the Coatings after the Immersion Test

Figure 9 shows the XRD patterns for the powders, as-sprayed coatings prepared onto JIS SS400 plates and the coatings after 24-h immersion test in the molten Al-45wt.%Zn alloy. The peaks from double carbides of Co_6W_6C and Co_3W_3C appeared in the WC/12 wt.% Co coating (HV-W1) after the immersion test. Co_6W_6C phase appeared in the WC/12 wt.% Co with low carbon coating (HV-W2) with Co_3W_3C phase originally existed in the powder. The peak intensities from double carbide tend to increase after the immersion test in the both WC/12 wt.% Co coatings. Considering that the formation of double carbide decreases the amount of reactive metal Co

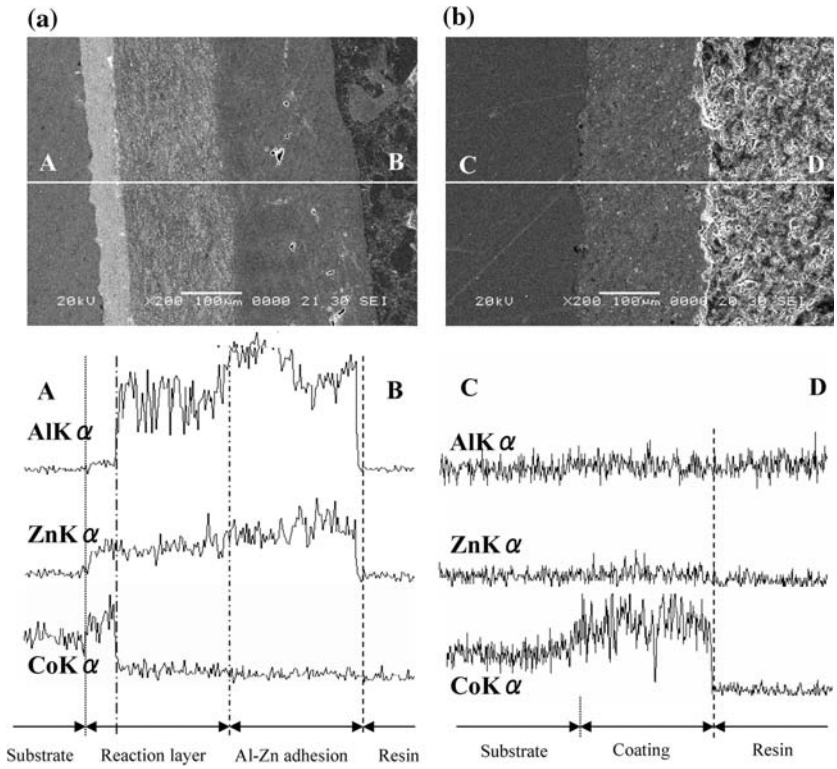

Fig. 8 EDX line analysis of the coatings after the immersion test in the molten Al-45wt.%Zn alloy. (a) WC/12 wt.% Co (HV-W1, 209 h), (b) MoB/CoCr (HV-B1, 623 h)

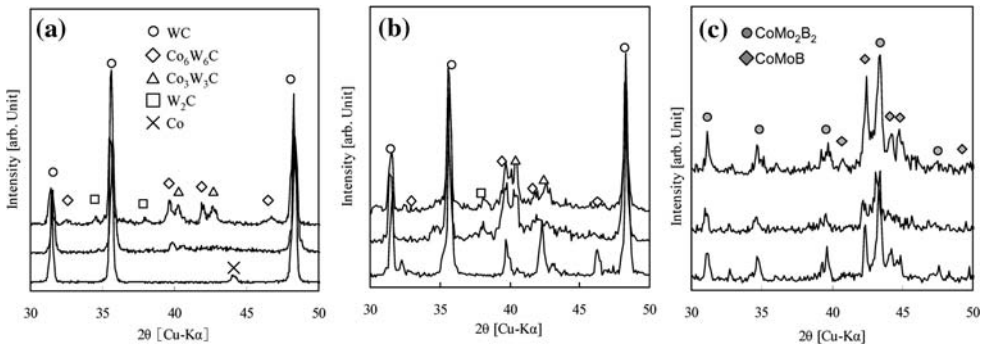

Fig. 9 XRD patterns for (a) WC/12 wt.% Co (HV-W1), (b) WC/12 wt.% Co with low carbon (HV-W2), and (c) MoB/CoCr (HV-B1). Bottom, middle, and top patterns in each figure correspond to powder, as-sprayed coating and the coating after 24-h immersion in the molten Al-45wt.%Zn alloy, respectively

(Ref 7), longer lifetime of the HV-W2 coating is reasonable. No clear change of the XRD patterns is observed even after the immersion test in the MoB/CoCr coating.

3.5 Optimization of the Coating Structure onto High CTE Substrate

Figure 10 shows measured expansion ratio of the AISI 316L as substrate and the spray coatings of Co-based alloy as undercoat and MoB/CoCr as topcoat, whose CTE values are summarized in Table 2. The AISI 316L substrate has the highest CTE of 19.3×10^{-6}/K and the MoB/CoCr coating has the lowest (9.2×10^{-6}/K). At first heating cycle, inflexion point with shrinkage is seen only in the thermal spray coatings about 900-1000 K.

The lifetime of the MoB/CoCr coatings in the molten Al-45wt.%Zn alloy is shown in Fig. 11. The coating onto AISI H13 (HV-B1) has no damage after long-term immersion of more than 600 h as mentioned previously. However, the HV-B2 coating with same coating thickness of HV-B1 has much lower lifetime of 213 h due to high CTE substrate of AISI 316L. This shows the large difference in the CTE between the substrate and the MoB/CoCr coating seriously affects the durability of the coating. It is

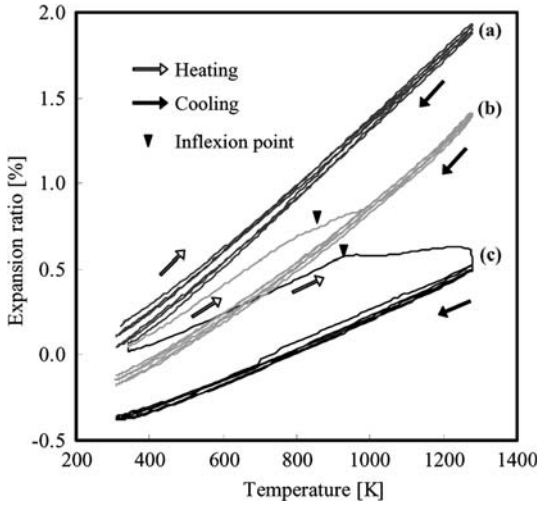

Fig. 10 Measured expansion ratio of (a) the AISI 316L as substrate and the spray coatings of (b) Co-based alloy as undercoat and (c) MoB/CoCr as topcoat

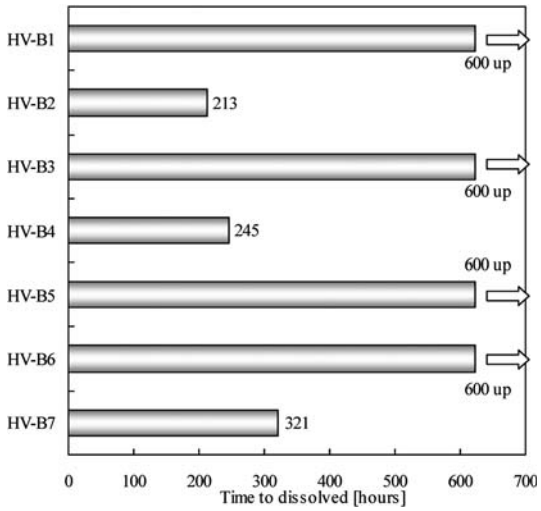

Fig. 11 Lifetime of the specimens coated onto AISI 316L in the molten Al-45wt.%Zn. HV-B1, B3, B5, and B6 specimens show no damage after about 600-h immersion test

considered that increase in the volume of the MoB/CoCr coating is relatively lower during immersion in the Al-45wt.%Zn alloy at 923 K. In contrast, stainless AISI316L substrate expands widely that causes the damage of the coating, such as cracks and peel off.

Although it is found that formation of undercoat by AISI 440C (50 μm in thickness) with an intermediate CTE of 12.4×10^{-6}/K is effective to improve lifetime (HV-B3: no damage after 600 h), martensitic steel of AISI 440C is difficult to apply to actual application due to its low durability in the molten alloy. Since Co-based alloy coating with the CTE of 15.3×10^{-6}/K has relatively higher durability compared to the AISI 440C coating, it seems to be suitable for undercoat. However, the lifetime is insufficient (HV-B4: 245 h) when thickness of undercoat and topcoat is same as that of HV-B3. The damage behavior was studied by micro-structural analysis to solve the problem of insufficient lifetime. Figure 12 shows optical micrographs of cross sections of the MoB/CoCr coating (HV-B4) after 245-h immersion test. A lot of cracks, delamination and peel off are observed at immersed area into the Al-45wt.%Zn alloy as shown in Fig. 12(a-c). Although Fig. 12(d) is no immersed area, cracks are generated in the MoB/CoCr coating. This result means that the mechanical damage of crack is generated by only heat-shock, not dissolution.

In the case of increasing undercoat thickness from 50 to 100 μm (HV-B5) or decreasing topcoat thickness from 150 to 100 μm (HV-B6), no damage is observed after 600-h immersion. As for HV-B7 with thicker undercoat of 500 μm, its lifetime becomes shorter of 321 h, where peeling at the interface between undercoat and substrate is observed. Therefore, HV-B5 (150 μm topcoat and 100 μm undercoat) and HV-B6 (100 μm topcoat and 50 μm undercoat) are the best coating structure within this study to reduce the negative influence of the large CTE difference.

4. Discussion

4.1 Erosion Resistance of MoB/CoCr Coating against Molten Al-45wt.%Zn

When applying thermal spray coatings to molten metal applications, high erosion resistance against molten metal is the most important property for the coating material. Mo-(Ni, Cr)-B cermet material, including ternary double boride of Ni-Mo-B, is known to have excellent durability against the molten aluminum (Ref 12, 13). Also, thermal-sprayed coating of the MoB/CoCr is mainly composed of ternary double boride of Co-Mo-B, where Co, instead of Ni (Ref 3), is selected to reduce the reactivity in the molten metal (Ref 14). Further, it is considered that the composition ratio of MoB and CoCr is also optimized in terms of lower content of reactive metal matrix, mainly Co. Therefore, the MoB/CoCr coating shows the excellent durability without the change of the crystal structure.

On the other hand, WC, not ternary compound, is dominant and content of double carbides of Co-W-C is lower in the as-sprayed WC/12 wt.% Co with low carbon coatings. Increase of double carbides (η-phase) during immersion shows reaction between WC and Co suggesting that double carbide is also relatively inert compared to WC. Therefore, double carbide-rich WC/Co coating with little WC crystal may have good erosion resistance. Since difference in reactivity between double boride of Co-Mo-B and double carbide of Co-W-C is presently unclear, basic investigation about reactivity of such ternary ceramics is future issues to find optimal composition. It is considered that Co-based alloy as metal matrix in the MoB/CoCr has higher durability than pure Co as metal matrix in the WC/12 wt.% Co coatings. This inertness of the metal

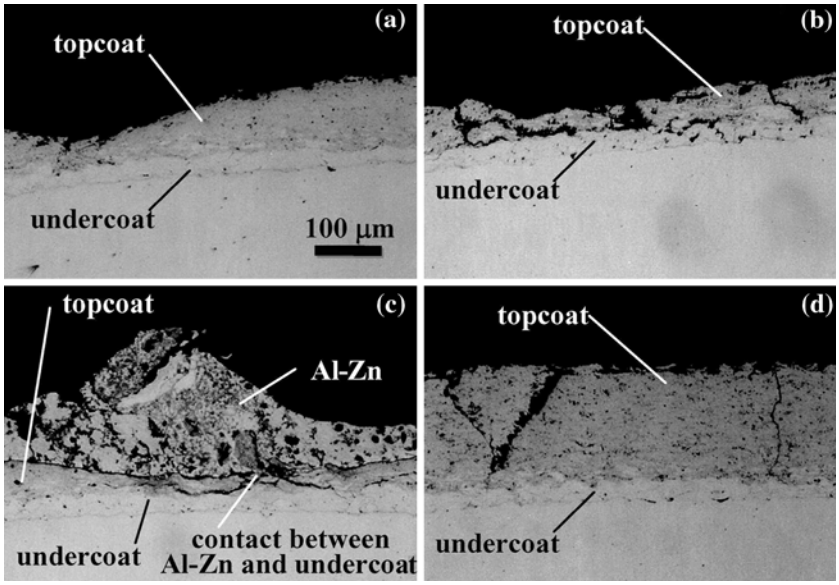

Fig. 12 Cross-sectional optical micrographs of the MoB/CoCr coating (HV-B4) after 245-h immersion test. (a, b, c) are immersed area and (d) is no immersed area near the center of the specimen

matrix may also contribute to good erosion resistance of the MoB/CoCr.

4.2 Heat-Shock Resistance of the MoB/CoCr Coating

Spray coatings for high temperature applications should have high heat-shock resistance to avoid mechanical damages, such as cracks and peel off. One of the possible characteristics to evaluate the heat-shock resistance is CTE of the coating. Additionally, small CTE difference between the coating and the substrate is an important factor to avoid damages. The behavior of expansion and shrinkage of the coating during the heating and cooling should be also considered. Thermal expansion curve in Fig. 10 shows that the thermal spray coatings have an inflexion point with shrinkage at 850-900 K of first heating cycle. After the shrinkage, thermal expansion curves become almost stable from first cooling to third cooling cycle. It is suggested that the shrinkage is caused by recrystallization of amorphous phase and/or relaxation of residual stress in the as-sprayed coating. Thus, it should be considered that the shrinkage of the spray coatings might negatively affect the heat-shock resistance of the coating in the molten Al-Zn alloy because its operating temperature is more than 900 K and substrate expands with increasing temperature. As a result, actual CTE difference between the coating and the substrate becomes larger than that of measured CTE difference. Posttreatment of heating to make shrinkage of the coatings will be necessary prior to operation in actual applications.

Ceramic or cermet coatings with relatively lower CTE are generally formed onto metal substrates with higher CTE in plasma and HVOF sprayings. This means that use of high CTE materials within ceramics or cermet is better to reduce the CTE difference between coating and substrate. As the CTE of MoB/CoCr is higher than that of WC/12 wt.% Co, influence of heat shock by the CTE difference should become smaller. In spite of higher CTE than that of MoB/CoCr, ceramic coating of ZrO_2-8 wt.% Y_2O_3 has shorter lifetime by crack generation showing that high fracture toughness is also required for the coating material. Therefore, it is likely that cermet material of MoB/CoCr is the most adaptable choice to obtain the required properties, such as higher inertness, relatively higher CTE and higher fracture toughness. In the case of WC/Co, both CTE and fracture toughness can become higher with increasing Co content that will attain higher heat-shock resistance. On the other hand, increasing Co content apparently degrades the erosion resistance. Decrease of Co content is also difficult to obtain all required properties.

4.3 Behavior of the Damage for the MoB/CoCr Coating

The results of cross-sectional analysis shown in Fig. 12 suggest the damage of the MoB/CoCr coating is mainly derived from insufficient heat-shock resistance due to large CTE difference between the coating and substrate. Although AISI316L substrate expands larger, expansion of the MoB/CoCr coating is smaller due to its lower CTE as well as shrinkage by recrystallization and relaxation of residual stress. As a result, vertical cracks seen in Fig. 12(d) are considered to be easily generated.

From the observation of crack generation at no immersed area in Fig. 12(d), it is easy to consider that cracks are also generated at immersed area by heat shock. After crack formation, the coating thickness becomes thinner

due to delamination as shown in Fig. 12(a, b). At last, when the undercoat or substrate is exposed to Al-Zn alloy directly or passing through the cracks as shown in Fig. 12(c), adhesion of the alloy is occurred and followed by dissolution of the specimen. In conclusion, optimization of coating structure including MoB/CoCr thickness as topcoat, undercoat material, undercoat thickness and thickness combination between top and undercoat will be essentially required when the MoB/CoCr coating is applied to actual application to attain intrinsic performance of inert MoB/CoCr.

5. Conclusions

The durability of the coatings prepared by thermal spraying has been investigated in the molten Al-45wt.%Zn alloy. The MoB/CoCr coatings has excellent durability in the molten Al-45wt.%Zn alloy compared to the conventional cermet coating of WC/12 wt.% Co as well as ceramic coatings of Al_2O_3 and ZrO_2-8wt.%Y_2O_3. The molten alloys are hard to adhere onto the coating surface of the MoB/CoCr. The crystal structure of the MoB/CoCr coating is mainly composed of the double borides, and little change of the structure is observed after immersion test, suggesting that the double borides have much higher durability against the molten alloys.

In order to apply to actual continuous dipping rolls by improving lifetime, using undercoat is effective to reduce the influence of large difference in thermal expansion between the MoB/CoCr coating and austenitic steel of stainless AISI 316L. It should be noted that optimized thickness combination of topcoat and undercoat is important.

Acknowledgment

The authors thank Mr. Isao Aoki, Mr. Satoshi Tawada, and Mr. Yoshiaki Hayashi for their technical support. The authors also thank Mr. Nobuaki Kato for his valuable suggestion.

References

1. J.R. Davis, Ed., *Handbook of Thermal Spray Technology*, ASM International, 2004, p 56-60, 62-70, 133-168
2. R.B. Heimann, Plasma-Spray Coating, Principles and Applications, VCH Verlagsgesellschaft mbH, Germany, 1996
3. K. Hamashima, Y. Shinozaki, and M. Sasaki, Thermal Spraying of Mo_2NiB_2-Ni Cermet, *Proc. International Conference on Powder Metallurgy & Particulate Materials, Advances in Powder Metallurgy & Particulate Materials*, part2, (Chicago, USA), Metal Powder Industries Federation and APMI International, 1997, p 43-48
4. H. Yamaguchi and T. Hisamatsu, Reaction Mechanism of the Sheet Galvanizing, *J. Iron Steel Inst. Japan*, (in Japanese) 1977, **63**(7), p 1160-1169
5. T. Tomita, Y. Takatani, Y. Kobayashi, Y. Harada, and H. Nakahira, Durability of WC/Co Sprayed Coatings in Molten Pure Zinc, *J. Iron Steel Inst. Japan Int.*, 1993, **33**(9), p 982-988
6. K. Tani, T. Tomita, Y. Kobayashi, Y. Takatani, and Y. Harada, Durability of Sprayed WC/Co Coatings in Al-added Zinc Bath, *J. Iron Steel Inst. Japan Int.*, 1994, **34**(10), p 822-828
7. A.J. Stavros, Behavior of Some Tungsten Carbide Coatings in Molten Zinc, *Proc. of 9th National Thermal Spray Conference*, C.C. Berndt, Ed., Oct 7-11 (Cincinnati, OH), ASM International, 1996, p 141-146
8. D. Nolan, P. Mercer, and M. Samandi, Reactivity of WC-12% Co Thermal Spray Powders with Molten Zinc Alloys as a Function of Phase Content, *Surface Modification Technologies XI*, T.S. Sudarshan, M. Jeandin, and K.A. Khor, Eds., The Institute of Materials, 1998, p 312-317
9. H. Mizuno, J. Kitamura, S. Osawa, and T. Itsukaichi, Development of Durable Spray Coatings in Molten Aluminum Alloy, *Proc. International Thermal Spray Conference 2005* (Basel, Switzerland), ASM International, 2005, CD-ROM
10. H. Mizuno, J. Kitamura, S. Tawada, and T. Itsukaichi, Development of Durable Spray Coating in Molten Al and Al-Zn alloys, *Proc. 1st Asian Thermal Spray Conference* (Nagoya, Japan), Asian Thermal Spray Committee, 2005, p 81-82
11. H. Mizuno, J. Kitamura, S. Tawada, and T. Itsukaichi, MoB/CoCr Spray Coating with Higher Durability in Molten Al and Al-Zn Alloys, *Proc. International Thermal Spray Conference 2006* (Seattle, USA), ASM International, 2006, CD-ROM
12. K. Hamashima and Y. Shinozaki, Development of the Thermal Spraying of Mo-Ni-B Cermet I: Preparation of Spraying Powder and Properties of its Films, Pre-Prints of the National Meeting of Japan Welding Society, Japan Welding Society, Vol. 62, 1998, p 154-155
13. K. Hamashima and Y. Shinozaki, Development of the Thermal Spraying of Mo-Ni-B Cermet II: Effects of the Heat Treatment on Properties of its Films, Pre-Prints of the National Meeting of Japan Welding Society, Japan Welding Society, Vol. 63, 1998, p 72-73
14. T. Itsukaichi and S. Osawa, US Patent 6984255